

Stability of rubidium molecules in the lowest triplet state

B. J. Verhaar and S. J. J. M. F. Kokkelmans

Eindhoven University of Technology, P.O. Box 513, NL-5600 MB Eindhoven, The Netherlands

(Received 12 March 2017; published 14 April 2017)

Experiments involving ultracold molecules require sufficiently long lifetimes, which can be very short for excited rovibrational states in the molecular potentials. For alkali-metal atoms such as rubidium, a lowest rovibrational molecular state can both be found in the electronic singlet and triplet configurations. The molecular singlet ground state is absolutely stable. However, the lowest triplet state can decay to a deeper bound singlet molecule due to a radiative decay mechanism that involves the interatomic spin-orbit interaction. We investigate this mechanism, and find the lifetime of rubidium molecules in the lowest triplet rovibrational state to be about 20 min.

DOI: [10.1103/PhysRevA.95.042706](https://doi.org/10.1103/PhysRevA.95.042706)

I. INTRODUCTION

Stable ultracold molecules are of high experimental and theoretical interest [1]. In particular molecules with a permanent electric dipole moment offer the opportunity to explore many-body states [2] that are impossible to reach with the isotropic nature of the short-range ultracold atomic interactions. One of the routes to create ultracold diatomic molecules is to associate them from ultracold atoms. Initially atoms are associated into weakly bound Feshbach molecules by sweeping a magnetic field across resonance. Subsequently stimulated Raman adiabatic passage (STIRAP) is performed on these molecules to convert them to the lowest state of a particular potential [3]. This technique has proven to be very efficient, and in 2008 the first sample of diatomic KRb molecules in the rovibrational ground state was produced [4]. More recently, this also succeeded for RbCs [5,6], which contrary to KRb is chemically stable under two-body collision processes [7]. Also nondipolar Rb₂ [8] and Cs₂ [9] ground-state molecules have been created in this way.

The stability of these molecules is crucial for experiments, and therefore it is only natural to create the molecules in the absolute ground state. This is the rovibrational ground state of the electron spin singlet potential $X^1\Sigma_g$. The singlet potential is energetically very deep, and to reach its ground state via STIRAP, typically an additional laser system is required. However, the lowest spin triplet state is much less deep, and can be reached more easily with the laser set-up which is usually present for laser cooling and trapping purposes.

While (singlet) ground-state molecules are absolutely stable with respect to radiative decay, molecules in the lowest triplet state are not. However, the question is whether the radiative lifetime will be a practical limiting factor to current experiments. Recent experimental and theoretical work shows that a gas of singlet ground-state molecules has a very short reactive lifetime resulting from three-body collisions [5,10]. Also, triplet molecules have theoretically been shown to be unstable towards trimer formation [11]. On the other hand, isolated Rb₂ molecules in the lowest triplet state, produced in an optical lattice [8], are not sensitive to other types of decay apart from the radiative process, and may potentially have a much longer lifetime than the reactive lifetimes of both singlet and triplet molecules in their lowest rovibrational state.

In this paper, we investigate the lifetime of the lowest triplet Rb₂ state $a^3\Sigma_u^+$. While our approach is generic for all

alkali-metal atoms, rubidium is particularly interesting as it is currently the most widely used species in ultracold quantum gas experiments. Our treatment applies to ⁸⁵Rb₂ and ⁸⁷Rb₂ molecules. Rb₂ molecules in the lowest triplet state are not absolutely stable, as the combined valence electron spins may form a lower energetic singlet configuration.

In the following we present a calculation of the lifetime of Rb₂ molecules in their lowest triplet state, considering the two most probable decay mechanisms involving a spin flip. The first mechanism we consider arises from the interatomic part V^{so} of the total spin-orbit interaction [12,13] that admixes a set of intermediate electronic states into the lowest triplet state. The spin flip is followed by $E1$ decay, and we show that this is the dominant mechanism that leads to a lifetime of about 20 min. The second mechanism starts with an energy-conserving spin flip, resulting from the magnetic dipole-dipole interaction, which is followed by nuclear spin $M1$ decay. This mechanism appears in practice to be completely negligible, as the associated lifetime is 10²⁹ s, and therefore leaves the interatomic spin-orbit mechanism as the sole mechanism responsible for the decay of rubidium molecules in the lowest triplet state. In both cases the two-atom system is considered to consist of two valence electrons 1,2 and two Rb⁺ ions A,B with nuclear spins i_A, i_B (see Fig. 1). In the following we focus on the ⁸⁷Rb₂ molecule for which $i_A = i_B (= \frac{3}{2})$.

II. INTERATOMIC SPIN-ORBIT COUPLING

One of the terms contributing to V^{so} in the situation of Fig. 1, in which the electron-ion pair 1,B of the dimer is involved is [12,13]

$$V^{so}(1,B) = \frac{e}{4m^2c^2} [\vec{E}(\vec{r}_{1B}) \times \vec{p}_1] \cdot \vec{\sigma}_1 \equiv \frac{e\hbar}{4m^2c^2} \vec{V}_{1B} \cdot \vec{\sigma}_1, \quad (1)$$

which includes the Thomas precession factor $\frac{1}{2}$. We define the shorthand notation \vec{V}_{1B} for the spatial part of $V^{so}(1,B)$, i.e., $\vec{E}(\vec{r}_{1B}) \times \vec{p}_1$ (similarly for other electron-ion combinations). In Eq. (1) the quantity $\vec{E}(\vec{r}_{1B}) = e\hat{r}_{1B}/(4\pi\epsilon_0r_{1B}^2)$ is the electric field operating on electron 1 due to the net charge of the other ion B^+ concentrated at its nucleus, \hat{r}_{1B} is the unit vector \vec{r}_{1B}/r_{1B} , $\vec{\sigma}$ the Pauli spin vector, \vec{p}_1 the electronic momentum operator, e the elementary charge, c the velocity of light, and m the electron mass. Rewritten in atomic units and including

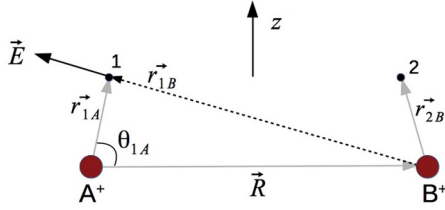


FIG. 1. Geometry of the Rb_2 molecule, considered to consist of two valence electrons 1,2, and two Rb^+ ions A^+, B^+ . Electrons 1,2 and the atomic nuclei are initially spin polarized in a direction z (nuclear spins i_A and i_B). Vector $\vec{E}(\vec{r}_{1B})$ is the Coulomb field at the position of electron 1 from the net charge of ion B^+ concentrated at nucleus B. The figure illustrates one of the four terms contributing to the interatomic spin-orbit interaction V_{fi}^{so} [see Eq. (4)].

the $2A$ term we find

$$V^{\text{so}}(1,B) + V^{\text{so}}(2,A) = \frac{1}{4} \left(\frac{\lambda_c}{a_0} \right)^2 (\vec{V}_{1B} \cdot \vec{\sigma}_1 + \vec{V}_{2A} \cdot \vec{\sigma}_2), \quad (2)$$

with λ_c the reduced electron Compton wavelength and a_0 the Bohr radius.

We study the excitation process at fixed values of the internuclear distance R in a range where it is reasonable to assume that electron 1 is in one atom and electron 2 in the other, which is roughly equal to or larger than twice the Rb atomic van der Waals radius $r_{\text{vdW}} = 5.72a_0$ [14]. Therefore, in connection with the positions of the electrons relative to ions A and B , we define a pair of projection operators Π on disjoint parts of the four-particle (two valence electrons and two ions) configuration space where either $1A, 2B$ is the composition of the two atoms (projection operator $\Pi_{1A,2B}$) or $1B, 2A$ ($\Pi_{1B,2A}$). We thus rewrite the above expression (2) as

$$V^{\text{so}} = \frac{1}{4} \left(\frac{\lambda_c}{a_0} \right)^2 [\Pi_{1A,2B} (\vec{V}_{1B} \cdot \vec{\sigma}_1 + \vec{V}_{2A} \cdot \vec{\sigma}_2) + \Pi_{1B,2A} (\vec{V}_{1A} \cdot \vec{\sigma}_1 + \vec{V}_{2B} \cdot \vec{\sigma}_2)]. \quad (3)$$

It is the $\vec{\sigma}_1 - \vec{\sigma}_2$ part V_{fi}^{so} of V^{so} , proportional to the difference of the valence electron spins (antisymmetric in 1 and 2), that admixes a superposition of *final* singlet two-particle electronic *sp* states into the fully spin-polarized initial dimer state $|\Psi_i\rangle$ before the decay:

$$V_{fi}^{\text{so}} = \frac{1}{8} \left(\frac{\lambda_c}{a_0} \right)^2 [\Pi_{1A,2B} (\vec{V}_{1B} - \vec{V}_{2A}) + \Pi_{1B,2A} (\vec{V}_{1A} - \vec{V}_{2B})] \cdot (\vec{\sigma}_1 - \vec{\sigma}_2). \quad (4)$$

Note that in the above we discuss operator equations which act on the combined Hilbert spaces of the spatial and spin degrees of freedom. Below, we will only regard the spin-antisymmetric part of the Hilbert space as the $\vec{\sigma}_1 + \vec{\sigma}_2$ part connects the initial state to states that do not contribute to the decay. The associated projection operators on spin-symmetric and spin-antisymmetric parts of Hilbert space commute with the projection operators $\Pi_{1A,2B}$ and $\Pi_{1B,2A}$ on configuration space and therefore the spin operators $(\vec{\sigma}_1 - \vec{\sigma}_2)$ can be pulled out of the square brackets.

For the initial and final electronic states we take the R -dependent adiabatic potential-energy curves (PECs) and

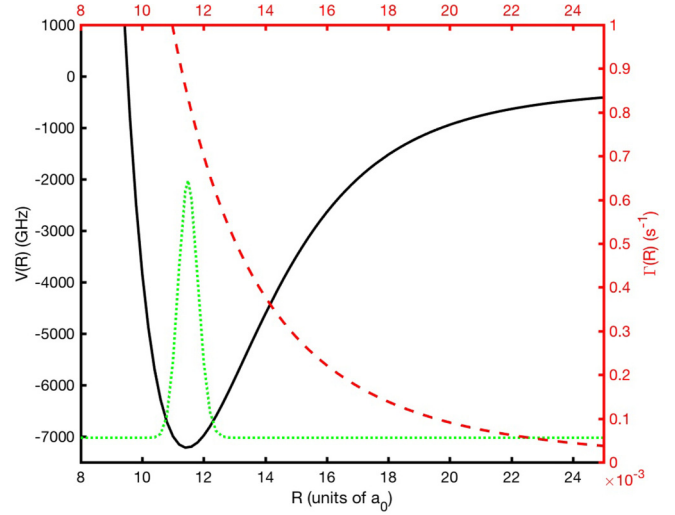


FIG. 2. Potential for lowest $\text{Rb}_2 0_u^-$ and 1_u states, where the rovibrational ground state is located at -7.026 GHz (solid black line). The corresponding squared wave function $[\phi_i(R)]^2$ is indicated (dotted green line). Also indicated is the local decay rate $\Gamma(R)$ (dashed red line).

electronic transition dipole moments (TDMs) of the low-lying Rb dimer states from Ref. [15]. These have been calculated both without and with (*intra*-)atomic spin-orbit coupling, leading to $\Lambda\Sigma$ states and Ω states, respectively. Here $\Lambda, \Sigma,$ and Ω are the projections of the total electron orbital, spin, and total angular momentum along the internuclear axis, respectively. Interatomic spin-orbit coupling is not taken into account (see also Refs. [16–18]). In our case the choice between the two types of states depends crucially on the range of interatomic distances where the initial state is concentrated. In Fig. 2 we present the PEC for the initial lowest triplet rovibrational state with quantum numbers $v_i, l, m_l = 0, 0, 0$, together with the corresponding eigenfunction squared $[\phi_i(R)]^2$ with a Gaussian-like shape, normalized according to $\int_0^\infty [\phi_i(R)]^2 dR = 1$. It is concentrated in the interval from $R = 10$ to $14 a_0$, which contributes dominantly to the transition from $|\Psi_i\rangle$ to the final electronic states via intermediate states, while the PECs for the $(1)0_u^-$ and $(1)1_u$ initial Ω states are virtually identical to those of the $a^3\Sigma_u^+$ state (for $R = 10$ to $14 a_0$ in six of eight decimals). For that reason we will only make use of the Ω -type TDMs in Ref. [15]. In addition, we only include them for *sp* final states and omit the *sd* states, which are not admixed by V^{so} .

In order to connect to the TDMs of Ref. [15] we now expand the factor $1/r_{1B}^3$ in the electric field $\vec{E}(\vec{r}_{1B}) = \vec{r}_{1B}/r_{1B}^3$ (similarly for other electric fields in the previous equations) in inverse powers of R , using the shorthanded notations $\rho = r_{1B}/R, p = -2 \cos \theta_{1A} r_{1A}/R, q = (r_{1A}/R)^2$:

$$\begin{aligned} 1/\rho^n &= 1 - \frac{n}{2}(p+q) + \frac{n(n+2)}{8}(p+q)^2 + \dots \\ &= 1 + n \frac{z'_{1A}}{R} - \frac{n}{2} \left(\frac{r_{1A}}{R} \right)^2 + \frac{n(n+2)}{2} \left(\frac{z'_{1A}}{R} \right)^2 + \dots \end{aligned} \quad (5)$$

We use a nuclei-fixed right-handed coordinate system: the origin halfway the nuclei [15], an internuclear z' axis, and a perpendicular pair of x' and y' axes with an arbitrary orientation around the z' direction. Furthermore, we neglect cross-terms between the intra- and interatomic spin-orbit couplings (both weak), so that the electronic momentum in Eq. (1) can be expressed as a commutator of the Hamiltonian H_{el} for the two valence electrons [15] with the position vector \vec{r}_{1A} : $\vec{p}_1 = i[H_{\text{el}}, \vec{r}_{1A}]$. As a consequence, we have

$$\vec{E}(\vec{r}_{1B}) \times \vec{p}_1 \propto [H_{\text{el}}, \vec{r}_{2B} \times \vec{r}_{1A}] = [H_{\text{el}}, -\vec{R} \times \vec{r}_{1A}], \quad (6)$$

i.e., only the component $\vec{r}_{1A\perp} = \vec{r}_{1\perp}$ perpendicular to \vec{R} and only even orders in the $1/\rho^3$ expansion survive. The zeroth-order contribution to \vec{V}_{1B} can thus be dealt with in terms of TDMs and the second-order term can be used to estimate the relative error, which turns out to be roughly $(r_{\text{vdW}}/R)^2 \approx 25\%$ in the relevant range $10 < R < 14a_0$ (see Fig. 2). This conclusion is valid for other electron-ion combinations, too.

A. Symmetry aspects

The foregoing steps change the spatial operator multiplying $\Pi_{1A,2B}$ in Eq. (4) into $\vec{V}_{1B} - \vec{V}_{2A} = -\frac{i}{R^3} \vec{R} \times [H_{\text{el}}, (\vec{r}_{1A} + \vec{r}_{2B})]$. A similar result is obtained for the operator multiplying $\Pi_{1B,2A}$. In total we obtain

$$V_{fi}^{\text{so}} = \frac{1}{8R^2} \left(\frac{\lambda_c}{a_0} \right)^2 \hat{R} \times (\Pi_{1A,2B}[H_{\text{el}}, \vec{r}_1 + \vec{r}_2] + \Pi_{1B,2A}[H_{\text{el}}, \vec{r}_1 + \vec{r}_2]) \cdot (\vec{\sigma}_1 - \vec{\sigma}_2), \quad (7)$$

with \hat{R} the unit vector \vec{R}/R .

The symmetry properties of this expression determine selection rules for the admixtures induced by V_{fi}^{so} . Splitting the electronic spatial part $\vec{D} = \vec{r}_{1\perp} + \vec{r}_{2\perp}$ of V_{fi}^{so} into spherical components $q = \pm 1$ [19], $D_{\pm 1'} = \mp(D_{x'} \pm iD_{y'})/\sqrt{2}$, we find that they change parity u into g and in addition change the z' component M'_L of the total electronic wave function by ± 1 , i.e., only a 1_g part is added to 0_u^- and only $0_g^+, 0_g^-, 2_g$ parts to 1_u . We also find that each of the $D_{\pm 1'}$ terms changes σ_v reflection parity [12] from $+$ to $-$ and vice versa. The foregoing implies that we can use the $\Delta\Omega = \pm 1$ transition dipole moments (TDMs) for $E1$ transitions published by Allouche *et al.* [15] to calculate the $(\vec{r}_1 + \vec{r}_2)_{\pm 1'}$ spatial matrix elements, in combination with the spin matrix elements $\langle (S, M'_S)_f = 0, 0 | (\vec{\sigma}_1 - \vec{\sigma}_2)_{\pm 1'} | (S, M'_S)_i = 1, \pm 1 \rangle$. The equality $q = M'_S$ illustrates angular momentum conservation along the z' symmetry axis: Spin angular momentum is transferred to orbital angular momentum.

A necessary following step is to impose Kronig symmetry [20]: We require invariance of the Hamilton operator under the combination of a rotation of the nuclei over π around the y' axis (leaving the electrons alone) and space inversion of the electronic position coordinates with respect to the origin. Both H_{el} and each of the $\Pi_{1A,2B}$ and $\Pi_{1B,2A}$ terms in Eq. (7) obey this invariance. Kronig symmetry of the Hamiltonian implies that the eigenstates have to be either symmetric or antisymmetric (Kronig symmetry type c or d in Herzberg's notation [12,21]), or can be chosen as such.

As a consequence transitions induced by V_{fi}^{so} take place between states with equal Kronig symmetry only. To find the c and d type $(1)0_u^-$ and $(1)1_u$ states we make use of our earlier conclusion that in the R interval of interest these Ω states are very close to ${}^3\Sigma_u^+$ states, i.e., $\Lambda\Sigma$ states with $\Lambda = 0$ and $S = 1, \Sigma = 0, \pm 1$. We therefore equate the latter to the corresponding Ω states:

$$\begin{aligned} |(1)0_u^- \rangle &= |(1)3\Sigma_u^+, \Omega = \Sigma = 0 \rangle \\ &= |c, (1)3\Sigma_u^+, S = 1, \Omega = 0 \rangle \end{aligned} \quad (8)$$

is a Kronig-symmetric state by itself, as indicated by the symbol “ c ”, whereas $|(1)3\Sigma_u^+, \Omega = 1 \rangle$ exists in two versions, one with c and one with d symmetry:

$$\begin{aligned} |{}_d^c, (1)1_u \rangle &= [|\Sigma^+, S = 1, \Omega = 1, \Sigma = +1 \rangle \\ &\pm |\Sigma^+, S = 1, \Omega = 1, \Sigma = -1 \rangle] / \sqrt{2}. \end{aligned} \quad (9)$$

We conclude that the above-mentioned selection rules have to be further specified: Allowed transitions are $(c, 0_u^-) \rightarrow (c, 1_g), (c, 1_u) \rightarrow (c, 0_g^+)$ or $(c, 2_g)$, and $(d, 1_u) \rightarrow (d, 0_g^-)$ or $(d, 2_g)$.

Each of the above c and d states (8) and (9), multiplied by $|S, M_{S_z} = 1, +1 \rangle$ with the z axis along the polarization direction, is present initially with probability $1/3$ before the excitation by V_{fi}^{so} and has the total form,

$$\begin{aligned} |\Psi_{i, n_i=1}(\vec{R}) \rangle &= |\psi_i(n_i = 1; R) \rangle |L, M_L = 0, 0 \rangle \\ &\otimes |S, M_S = 1, +1 \rangle. \end{aligned} \quad (10)$$

The state $|\psi_i(n_i; R) \rangle$ stands for the R -dependent part of the initial adiabatic state of the valence electrons (eigenstates of H_{el} with serial number n_i of the corresponding eigenvalues counting from below) that defines their motion relative to the body-fixed axes. The states $|L, M_L \rangle$ specify the rotational motion of these axes relative to the space-fixed coordinate system. We leave out the nuclear spin state $|I, M_I = i_A + i_B, i_A + i_B \rangle$, which is not affected in the excitation and subsequent decay process for the present mechanism. As a further step we expand the initial electronic spin state in states $|1, M'_{S_z'} \rangle$ quantized along the direction of the z' axis:

$$|S, M_{S_z} = 1, +1 \rangle = \sum_{M'_{S_z'}} D_{1, M'_{S_z'}}^* (\phi_R, \theta_R, \chi_R) |1, M'_{S_z'} \rangle, \quad (11)$$

where $M'_{S_z'} = 0, \pm 1$ and $D_{1, M'_{S_z'}}^S$ is a rotation matrix element [19].

Each of the final states has the form,

$$\begin{aligned} |\Psi_{f, n_f}(\vec{R}) \rangle &= |\psi_f(n_f; R) \rangle, \\ |L' = 1, M'_{L_z'}; S', M'_{S_z'} = 0, 0 \rangle, \end{aligned} \quad (12)$$

with $|\psi_f(n_f; R) \rangle$ the final valence electron state and $L', M'_{L_z'}; S', M'_{S_z'}$ the rotational and spin angular momentum quantum numbers with components along the body-fixed z' axis in the final state. For each R value the states $|\psi_i(n_i; R) \rangle$ and $|\psi_f(n_f; R) \rangle$ form both an orthonormal set of eigenstates of the Hamiltonian H_{el} for the valence electrons.

B. Transition amplitudes and decay rate

For given \vec{R} and M'_S we now consider the transition amplitude induced by V_{fi}^{so} between an initial state $\Psi_{i,n_i}(\vec{R})$ and a final state $\Psi_{f,n_f}(\vec{R})$, divided by their energy difference:

$$A_{f n_f, i n_i}(M'_S, R) = \frac{\langle \Psi_{f n_f}(\vec{R}) | V_{fi}^{so} | \Psi_{i n_i}(\vec{R}) \rangle}{E_{f n_f} - E_{i n_i}}. \quad (13)$$

The energies E are R -dependent adiabatic potential-energy values [eigenvalues of H_{e1} ; see potential energy curves (PECS) in Ref. [15]]. Substituting Eq. (4) for V_{fi}^{so} and letting H_{e1} operate to the left in one term of the commutators and to the right in the other, we find that this results in a factor $E_{f n_f} - E_{i n_i}$ that cancels out the denominator in the above equation. Using the orthogonality of the D functions we find

$$A_{f n_f, i n_i}(M'_S, R) = \frac{1}{4\sqrt{3}R^2} \left(\frac{\lambda_c}{a_0} \right)^2 a_{f,i} b_{f,i}, \quad (14)$$

in which $a_{f,i}$ and $b_{f,i}$ are spatial and spin matrix elements:

$$\begin{aligned} a_{f,i} &= \langle \psi_f(n_f; R) | r_{1,+1} | \psi_i(n_i; R) \rangle \equiv \mathcal{D}_T(f n_f, i n_i), \\ b_{f,i} &= \langle 0,0 | (\vec{\sigma}_1 - \vec{\sigma}_2)_{-1} | 1,+1 \rangle = -2. \end{aligned} \quad (15)$$

Like the previous PECs, the transition dipole moments (TDMs) were tabulated by Allouche and Aubert-Frécon [15]. For comparison reasons, we discuss now an alternative approach that we investigated, which is, however, much less precise. We started from the full interatomic spin-orbit interaction V^{so} of Eq. (3) operating on the initial state (10), in which we took the radial wave function of the Rb $5s$ valence electron from [22], leading to a sum of $\Lambda S \Sigma \pi_e = 100g$ and $11 - 1g$ parts. Subsequently, we followed [23] in describing the $E1$ decay. The sum of the intraatomic spin-orbit couplings and the interatomic electric dipole-dipole interaction V^{dd} , which are valid for larger distances than considered up to now was diagonalized in the 18-dimensional space, leading to a set of 18 R -dependent eigenstates in the $5s5p$ space considered in Ref. [15], comparable to the final states $\psi_f(n_f; R)$ above. The main shortcoming of this approach is the role of the interaction V^{dd} in the radial range $10-14a_0$, where it is a bad approximation. Due to the strong repulsion in some of the final states and a strong attraction in the remaining ones the radial wave functions have small values. This leads to a lifetime of the lowest-energy Rb₂ triplet state of about 25 h, which is two orders of magnitude larger than what we calculate below.

Continuing the present treatment based on Ref. [15], we take the absolute square of the above amplitude A in Eq. (13) and integrate over the Euler angles. We thus find

$$\begin{aligned} & |A_{f n_f, i n_i}(M'_S, R)|^2 \sin(\theta_R) d\phi_R d\theta_R d\chi_R \\ &= \frac{1}{4R^4} \frac{8\pi^2}{3} \left(\frac{\lambda_c}{a_0} \right)^4 [\mathcal{D}_T(f, n_f; i, n_i; R)]^2. \end{aligned} \quad (16)$$

In our notation the TDM matrix element in this equation is given by

$$\mathcal{D}_T(f n_f, i n_i; R) = |\langle \psi_f(n_f; R) | [\vec{r}_{1q} + \vec{r}_{2q}] | \psi_i(n_i; R) \rangle|, \quad (17)$$

with the spherical component $q = \Omega_f - \Omega_i$, the change of the Ω values from initial to final states. The actual TDM values [15] show which final states are primarily excited starting

from the three initial states. For larger R (beyond $40a_0$) only the three lowest-energy $c, 1g$ states are significantly excited from 0_u^- , as well as the (2)-(3) 0_g^+ and (1) 2_g state from 1_u [for notation see [15]; (1) 0_g^+ = absolute singlet ground state]. More relevant for our purpose, in the above-mentioned interval $R = 10$ to $14 a_0$ the V_{fi}^{so} strength is distributed among transitions from 0_u^- to the sp states (1)-(2) 1_g , as well as from 1_u to (2)-(3) 0_g^+ , to (1)-(2) 0_g^- , and to (1) 2_g . All of these sp states undergo $E1$ decay back to the ss states.

Averaging over the three initial i, n_i states (8), (9), summing over the final f, n_f states, and multiplying by the average $\gamma = 3.60 \times 10^7 \text{ s}^{-1}$ of the Rb atomic first excited $^2P_{1/2}$ and $^2P_{3/2}$ spontaneous $E1$ decay rates, we find our estimate of the local decay rate $\Gamma(R)$ of the lowest triplet Rb₂ state,

$$\begin{aligned} \Gamma(R) &= \gamma \frac{1}{4R^4} \frac{8\pi^2}{3} \left(\frac{\lambda_c}{a_0} \right)^4 \sum_{i n_i} \sum_{f n_f} \left(\frac{1}{3} \delta_{i, 0_u^-} + \frac{2}{3} \delta_{i, 1_u} \right) \\ &\quad \times [\mathcal{D}_T(f n_f, i n_i; R)]^2, \end{aligned} \quad (18)$$

displayed in Fig. 2, and the total decay rate for mechanism I,

$$\Gamma^I = \int_0^\infty \langle \phi_i(R) | \Gamma(R) | \phi_i(R) \rangle dR. \quad (19)$$

Our result for the total decay rate is $0.78 \times 10^{-3} \text{ s}^{-1}$, corresponding to a lifetime of about $1200 \text{ s} = 20 \text{ min}$.

III. MAGNETIC DIPOLE-DIPOLE INTERACTION

A second decay mode is a relaxation process predicted and evaluated (see [24,25]), after the first proposal of a magnetic trap for wall-free confinement of ultracold atoms by Pritchard [26] and specifically for spin-polarized hydrogen atoms by Hess [27]. The latter trap was experimentally realized by Hess *et al.* [28]. The predicted decay process is induced in two-body atomic collisions. It played a crucial role as a loss process in connection with the first realization of Bose-Einstein condensation in an ultracold gas of Rb rather than H by Wieman and Cornell *et al.* [29] in 1995 after the prediction [30] that ^{87}Rb rather than the more easily available ^{85}Rb isotope was the preferable isotope because of its positive scattering length in atom-atom scattering. Soon after that Ketterle *et al.* [31] were successful in creating Bose-Einstein condensation in an ultracold gas of spin-polarized Na atoms.

Bose-Einstein condensates in magnetic traps have macroscopic linear dimensions (0.01–1 mm). In this paper, however, we discuss the stability of pairs of Rb atoms bound in Rb₂ molecules and thus confined to a spatial region with linear size roughly a factor 10^6 smaller (see probability distribution displayed in Fig. 2). Due to this compact nature of the Rb₂ molecule in the lowest triplet states the influence of the above-mentioned long-range (R^{-3}) magnetic dipole-dipole interaction V^{dd} (as well as in the radiative decay to be discussed later) is reduced to a considerable extent. Moreover, for Rb₂ molecules doubly polarized along an axis z the stronger part of this interaction, $V^{dd(e,e)}$, among the valence electrons does not lead to a final state that contains an excited singlet component giving rise to decay. However, turning to the weaker part $V^{dd(e,n)}$, acting between the spin magnetic moment μ_e of the

electron of one atom and the nuclear spin magnetic moment μ_n at the nucleus in the other atom, the situation is different.

Consider, for instance, the pair 1, B in Fig. 1. The corresponding term in $V^{\text{dd}(e,n)}$ is

$$C \frac{3(\vec{\sigma}_1 \cdot \vec{r}_{1B})(\vec{\sigma}_B \cdot \vec{r}_{1B}) - r_{1B}^2 \vec{\sigma}_1 \cdot \vec{\sigma}_B}{r_{1B}^5}, \quad (20)$$

with $C = (\mu_0/4\pi)\mu_e\mu_n$. We now follow the procedure of expansion Eq. (6), but now for $n = 5$. In the present case only even terms contribute to the final result. For our estimate we keep only the zeroth-order term, implying that we simply replace \vec{r}_{1B} by $\vec{r}_{AB} = -\vec{R}$. This leads to the expression,

$$C \frac{3(\vec{\sigma}_1 \cdot \hat{R})(\vec{\sigma}_B \cdot \hat{R}) - \vec{\sigma}_1 \cdot \vec{\sigma}_B}{R^3}, \quad (21)$$

with the unit vector $\hat{R} = \vec{R}/R$ as in Eq. (7). The total expression is

$$V^{\text{dd}(e,n)} = C \frac{3(\vec{\sigma}_1 \cdot \hat{R})(\vec{\sigma}_B \cdot \hat{R}) - \vec{\sigma}_1 \cdot \vec{\sigma}_B + (1B \rightarrow 2A)}{R^3} + C \frac{(1B2A \rightarrow 1A2B)}{R^3}. \quad (22)$$

Here $(1B \rightarrow 2A)$ and $(1B2A \rightarrow 1A2B)$ stand for their preceding term but with the replacements indicated. The vectors $\vec{\sigma}_J (J = A, B)$ are dimensionless spin vectors, defined by the expression for the nuclear spin magnetic moments: $\vec{\mu}_n = \mu_n \vec{\sigma}_J$. The latter expression for $V^{\text{dd}(e,n)}$ is identical to the zeroth-order expression for the interatomic magnetic-dipole coupling between the spins of two valence electrons in diatomic molecules given in Eq. (3-2-34) on page 108 of Ref. [12]. In that paper the expression is worked out for the $S = 1 \rightarrow 1$ transition, whereas our interest is in the $S = 1 \rightarrow 0$ transition to singlet states which finally decay radiatively to the singlet $5s^2$ ground state.

Our initial state is again that given in Eq. (10), but now completed with the nuclear spin factor $|I, M_I, M_{Iz} = 3, +3\rangle$, which in this second mechanism plays a role, too:

$$|\Psi_{i,n_i=1}(\vec{R})\rangle = |\psi_i(n_i = 1; R)\rangle \otimes |L, M_L = 0, 0; S, M_S = 1, +1; I, M_{Iz} = 3, +3\rangle. \quad (23)$$

The operator $V^{\text{dd}(e,n)}$ does indeed admix excited electronic singlet states in this initial spin-polarized Rb_2 triplet state, via a term antisymmetric in the valence electron spins proportional to the difference of Pauli spin vectors $\Delta\vec{\sigma}_{12} = \vec{\sigma}_1 - \vec{\sigma}_2$, which is automatically also nuclear spin antisymmetric and proportional to $\Delta\vec{\sigma}_{AB} = \vec{\sigma}_A - \vec{\sigma}_B$. Only their -1 spherical components contribute. We refer to this part as $V_{fi}^{\text{dd}(e,n)}$, because it couples spin-symmetric initial triplet states to final singlet states before the decay. To simplify the notation we make use of the previous projection operators Π and introduce the rank 2 spherical tensors $S^{(2)}$ and $R^{(2)}$, each built from products of two spherical vectors:

$$R^{(2)}(\hat{R}\hat{R})_2, S^{(2)} = (\Delta\vec{\sigma}_{12}\Delta\vec{\sigma}_{AB})_2. \quad (24)$$

Then $V_{fi}^{\text{dd}(e,n)}$ can be expressed in terms of the product $R_{+2}^{(2)} \cdot S_{(-2)}^{(2)}$. We thus obtain the expression,

$$V_{fi}^{\text{dd}(e,n)} = -\frac{C}{R^3} (\Pi_{1A,2B} - \Pi_{1B,2A}) R_2^{(2)} \cdot S_{-2}^{(2)}, \quad (25)$$

for the magnetic dipole-dipole coupling inducing the transition to the final singlet states before the radiative decay.

In analogy to Eq. (12), the possible final states are

$$|\Psi_{f,n_f}(\vec{R})\rangle = |\psi_f(n_f; R)\rangle, \\ |L', M'_L = +2, +2; S', M'_S = 0, 0; I', M'_I = 2, +2\rangle, \quad (26)$$

with $|\psi_f\rangle$ one of the $5s^2$ states. Contrary to the situation for mechanism II, it is preferable in this case to use magnetic quantum numbers for the final states along the prepared polarization direction z . In Eq. (26) f is equal to 0_u^- (automatically of Krong symmetry-type c) or to $c, 1_u$, whereas the serial number n_f is any positive integer value in the discrete spectrum of the 0_u^- potential (continuum states will play a negligible role). The corresponding rotational angular momentum matrix elements are

$$\langle L', M'_L = 2, +2 | R_{+2}^{(2)} | L, M_L = 0, 0 \rangle = \sqrt{\frac{8}{15}}. \quad (27)$$

Splitting the $S^{(2)}$ spin matrix element in two, we have

$$\langle S', M'_S = 0, 0 | (\Delta\vec{\sigma}_{12})_{-1} | S, M_S = 1, +1 \rangle = -4, \\ \langle I', M'_I = 2, +2 | (\Delta\vec{\sigma}_{AB})_{-1} | I, M_I = 3, +3 \rangle = -\frac{2}{i_A} \\ = -\frac{4}{3}. \quad (28)$$

We apply the previous Eqs. (27) and (28) to calculate the transition amplitude A :

$$A_{f n_f, i n_i}(R) = \frac{\langle \Psi_{f,n_f}(\vec{R}) | V_{fi}^{\text{dd}(e,n)} | \Psi_{i,n_i}(\vec{R}) \rangle}{E_{f,n_f} - E_{i,n_i}} \\ = -\frac{32}{3} \sqrt{\frac{2}{15}} \frac{C}{R^3} \frac{\langle \psi_f(n_f; R) | \psi_i(n_i; R) \rangle}{E_{f,n_f} - E_{i,n_i}}. \quad (29)$$

The result no longer depends on the direction of \vec{R} . Note also that $V_{fi}^{\text{dd}(e,n)}$ in Eq. (25) does not affect the initial radial function $\psi_i(n_i; R)$, hence the inner product of ψ states in Eq. (29).

The next step is to derive the radiative decay rate for each of the states $|\Psi_{f,n_f}\rangle$ to the states of $c, 0_g^+$ symmetry type. Only the $c, 1_u$ states can decay electromagnetically: The 0_u^- state and the other 1_u state have Krong symmetry-type d . The multipole that is responsible for this decay has to satisfy several conditions. The spatial electronic part $(5s)^2$ of the Ψ_{f,n_f} states should not be changed, nor should the spin part $S = 0$: Both are already identical to the corresponding parts in the Rb_2 ground state. The only degrees of freedom susceptible to change are those of the ions, i.e., in particular the nuclei: in Eq. (26) the nuclear spin part $I', M'_I = 2, +2$ and the rotational part $L', M'_L = 2, +2$. The multipole that will lead to the required intervention should also be symmetrical in the nuclei. The foregoing conditions are satisfied by the spherical component along the (body-fixed) z' axis of a magnetic quadrupole:

$$(M2)_{2\mu_{z'}} = \frac{3}{2} \delta_{\mu_{z'}, 0} \mu_n R_{z'} (\sigma_{Az'} - \sigma_{Bz'}). \quad (30)$$

This component of a *molecular* magnetic quadrupole moment is indeed symmetrical in the nuclei, since $R_{z'} = z'_B - z'_A$ (see Fig. 1). It arises from the distribution of nuclear magnetization in the Rb_2 molecule relative to the total center of mass and relative to the body-fixed axes. While the structure of the above expression (30) can be understood from the foregoing conditions, its normalization can be obtained from the analogous expression for the *electron* spin quadrupole moment in diatomic molecules given in Ref. [32], Eq. (39).

The local decay rate $\Gamma(R)$ and the total decay rate Γ are therefore proportional to μ_n^4 , which already suggests an extremely small value for the total decay rate Γ . In more detail we have, using Eq. (27) in the same paper [32],

$$\begin{aligned} \Gamma_{f,n_f}(R) &= |A_{fn_f, in_i=1}|^2 \frac{1}{30} \frac{\mu_0}{4\pi\hbar} \\ &\times \sum_{L''M_L'', I''M_I'', n_f''} [\Delta E_{L'I'n_f'', L''I''n_f''}(R)/(\hbar c)]^5 \\ &\times |\langle L'', M_L''; I'', M_I'' | (M2)_{2,0_{z'}} | L', M_L'; I', M_I' \rangle|^2, \end{aligned} \quad (31)$$

with $L', M_L' = 2, +2, I', M_I' = 2, +2, n_f'' = n_f'$, and $\Delta E_{L'I'n_f'', L''I''n_f''}(R) = E_{L'I'n_f''}(R) - E_{L''I''n_f''}(R)$.

For our purpose it suffices to derive an upper limit. Our strategy is to overestimate all factors on the right-hand side of Eq. (31), including the $1/[E_{f,n_f} - E_{i,1}]^2$ factor in $|A|^2$, but excluding the factor $|\langle \psi_f(n_f; R) | \psi_i(n_i; R) \rangle|^2$ with $n_i = 1$ in $|A|^2$. The latter factor would have been the most difficult to evaluate, but can now be dealt with easily as will be shown below. We overestimate the energy numerator and underestimate the denominator. The former can be equated to the fifth power of the dissociation energy D_{eS} of the singlet ground state and the denominator to the square of half the energy difference of the nearest pair of subsequent $L = 2$ vibrational singlet levels. We denote the latter as ΔE_{n_f} , which is estimated in terms of the classical relative radial velocity (expressed in the maximum kinetic energy) and twice the radial distance R covered by the atoms during one period as $h\nu_{\text{vib}} = 3.2 \times 10^{-21} \text{ J}$. A strong magnetic field could in principle be helpful via the downward Zeeman shift of the triplet levels, but is too weak in practice ($1.855 \times 10^{-23} \text{ B J}$ for all alkali-metal species with B in Tesla). Finally, taking into account that the R interval of interest is between 10 and $14a_0$ we replace the factor $(1/R^4)a_0^{-4}$ by choosing $R_0 = 10a_0$ to be its maximum value 10^{-4} in atomic units. This implies that the local and the total decay rates become equal. We thus find

$$\Gamma^{\text{II}} = \Gamma^{\text{II}}(R_0) = \sum_{n_f} |A_{fn_f, in_i=1}(R_0)|^2 P_{fn_f}(R_0). \quad (32)$$

Here, $P_{fn_f}(R)$ is the decay rate for the state $|\Psi_{f,n_f}\rangle$ as if that were the initial state. We use Eq. (27) of Ref. [32] for the decay

rate induced by a magnetic quadrupole moment. Substituting the above expression, we find

$$\Gamma^{\text{II}} = \sum_{n_f} \langle \Psi_{f,n_f} | M_{2,0_{z'}}^\dagger M_{2,0_{z'}} | \Psi_{f,n_f} \rangle. \quad (33)$$

The product $M_{2,0_{z'}}^\dagger M_{2,0_{z'}}$ can be simplified using $\sigma_{Az'}\sigma_{Az'} = \sigma_{Bz'}\sigma_{Bz'} = 1$ and the anticommutation relation of the $\sigma_{Az'}$ and $\sigma_{Bz'}$ matrices, $[\sigma_{Az'}, \sigma_{Bz'}]_+ = 0$. The result is $M_{2,0}^\dagger M_{2,0} = 2(\frac{3}{2}\mu_n R_0)^2$. Finally, the remaining summation over n_f can be handled by means of the completeness relation,

$$\sum_{n_f} |\psi_f(n_f; R_0)\rangle \langle \psi_f(n_f; R_0)| = 1, \quad (34)$$

leading to

$$\begin{aligned} \Gamma^{\text{II}} &< \frac{2^9 10^{-4}}{15^2 \hbar} \left(\frac{D_{eS}}{\hbar c} \right)^5 \left(\frac{\frac{\mu_0}{4\pi} \mu_e \mu_n \mu_n}{\frac{1}{2} \Delta E_{n_f}} \right)^2 \\ &= 0.4 \times 10^{-68} \text{ s}^{-1}, \end{aligned} \quad (35)$$

corresponding to a lifetime of $2.5 \times 10^{68} \text{ s}$.

IV. CONCLUSION

We conclude that isolated rubidium molecules in the lowest-energy triplet state have a finite lifetime. This is due to a radiative mechanism involving an interatomic spin-orbit interaction and inducing decay to the singlet state. The lifetime is about 20 min, which is much longer than typical experimental time scales needed to study these ultracold molecules, created in an optical lattice starting from two atoms on each lattice site. We also studied a second mechanism induced by a magnetic dipole coupling between the valence electron spin of one atom and the nuclear spin of the other, followed by a magnetic quadrupole ($M2$) radiative transition to the $(1)c, 0_g^+$ ground state with a probability containing an additional factor μ_n^2 . This second mechanism leads to a lifetime that exceeds the earlier lifetime by at least a factor 1×10^{65} , and can therefore be completely disregarded. Other decay mechanisms resulting in a transition to deeper-bound singlet states involve collisions, for instance, with other triplet ground-state molecules [11]. Future experiments should be able to investigate this mechanism, and shed more light on the collisional lifetime.

ACKNOWLEDGMENTS

We gratefully acknowledge discussions with William Stwalley and Andrei Derevianko. This research was financially supported by the Netherlands Organisation for Scientific Research (NWO), and in part by the National Science Foundation under Grant No. NSF PHY11-25915.

[1] L. D. Carr, D. DeMille, R. V. Krems, and J. Ye, *New J. Phys.* **11**, 055049 (2009).

[2] A. Micheli, G. Pupillo, H. P. Büchler, and P. Zoller, *Phys. Rev. A* **76**, 043604 (2007).

- [3] S. J. J. M. F. Kokkelmans, H. M. J. Vissers, and B. J. Verhaar, *Phys. Rev. A* **63**, 031601(R) (2001).
- [4] K.-K. Ni, S. Ospelkaus, M. H. G. de Miranda, A. Pe'er, B. Neyenhuis, J. J. Zirbel, S. Kotochigova, P. S. Julienne, D. S. Jin, and J. Ye, *Science* **322**, 231 (2008).
- [5] T. Takekoshi, L. Reichsöllner, A. Schindewolf, J. M. Hutson, C. R. Le Sueur, O. Dulieu, F. Ferlaino, R. Grimm, and H.-C. Nägerl, *Phys. Rev. Lett.* **113**, 205301 (2014).
- [6] P. K. Molony, P. D. Gregory, Z. Ji, B. Lu, M. P. Köppinger, C. R. Le Sueur, C. L. Blackley, J. M. Hutson, and S. L. Cornish, *Phys. Rev. Lett.* **113**, 255301 (2014).
- [7] P. S. Żuchowski and J. M. Hutson, *Phys. Rev. A* **81**, 060703(R) (2010).
- [8] F. Lang, K. Winkler, C. Strauss, R. Grimm, and J. Hecker Denschlag, *Phys. Rev. Lett.* **101**, 133005 (2008).
- [9] J. G. Danzl, M. J. Mark, E. Haller, M. Gustavsson, R. Hart, J. Aldegunde, J. M. Hutson, and H.-C. Nägerl, *Nat. Phys.* **6**, 265 (2010).
- [10] M. Mayle, G. Quéméner, B. P. Ruzic, and J. L. Bohn, *Phys. Rev. A* **87**, 012709 (2013).
- [11] M. Tomza, K. W. Madison, R. Moszynski, and R. V. Krems, *Phys. Rev. A* **88**, 050701 (2013).
- [12] M. Mizushima, *The Theory of Rotating Diatomic Molecules*, 1st ed. (Wiley and Sons, New York, 1975).
- [13] T. Itoh, *Rev. Mod. Phys.* **37**, 159 (1965).
- [14] M. Mantina, A. C. Chamberlin, R. Valero, C. J. Cramer, and D. Truhlar, *J. Phys. Chem. A* **113**, 5806 (2009).
- [15] A.-R. Allouche and M. Aubert-Frécon, *J. Chem. Phys.* **136**, 114302 (2012).
- [16] A. R. Allouche, G. Nicolas, J. C. Barthelat, and F. Spiegelmann, *J. Chem. Phys.* **96**, 7646 (1992).
- [17] W. Mueller, J. Flesch, and W. Meyer, *J. Chem. Phys.* **80**, 3297 (1984).
- [18] W. Mueller and W. Meyer, *J. Chem. Phys.* **80**, 3311 (1984).
- [19] D. Brink and G. Satchler, *Angular Momentum*, 3rd ed. (Clarendon Press, Oxford, 2015).
- [20] R. d. L. Kronig, *Band Spectra and Molecular Structure* (Cambridge University Press, London, 1930).
- [21] G. Herzberg, *Molecular Spectra and Molecular Structure, I: Spectra of Diatomic Molecules* (Van Nostrand, Princeton, 1939).
- [22] L. Szasz and G. McGinn, *J. Chem. Phys.* **47**, 3495 (1967).
- [23] M. Movre and G. Pichler, *J. Phys. B* **10**, 2631 (1977).
- [24] A. Legendijk, I. F. Silvera, and B. J. Verhaar, *Phys. Rev. B* **33**, 626(R) (1986).
- [25] R. M. C. Ahn, J. P. H. W. v. d. Eijnde, and B. J. Verhaar, *Phys. Rev. B* **27**, 5424 (1983).
- [26] D. E. Pritchard, *Phys. Rev. Lett.* **51**, 1336 (1983).
- [27] H. F. Hess, *Phys. Rev. B* **34**, 3476 (1986).
- [28] H. F. Hess, G. P. Kochanski, J. M. Doyle, N. Masuhara, D. Kleppner, and T. J. Greytak, *Phys. Rev. Lett.* **59**, 672 (1987).
- [29] M. Anderson, J. Ensher, M. Matthews, C. Wieman, and E. Cornell, *Science* **269**, 198 (1995).
- [30] J. R. Gardner, R. A. Cline, J. D. Miller, D. J. Heinzen, H. M. J. M. Boesten, and B. J. Verhaar, *Phys. Rev. Lett.* **74**, 3764 (1995).
- [31] K. B. Davis, M.-O. Mewes, M. R. Andrews, N. J. van Druten, D. S. Durfee, D. M. Kurn, and W. Ketterle, *Phys. Rev. Lett.* **75**, 3969 (1995).
- [32] M. Mizushima, *Phys. Rev.* **134**, A883 (1964).